

Air flow analysis of 20 hp three phase induction motor

Anuprita Bhosale^{1,2}, Sathyanarayanan Nandagopal³ , Davidson Jebaseelan¹, Siva Kumar Ramasami¹, and Lenin Natesan Chokkalingam^{4,*}

¹ School of Mechanical Engineering, Vellore Institute of Technology, Chennai, India

² Veermata Jijabai Technological Institute, Mumbai, India

³ School of Electrical Engineering, Vellore Institute of Technology, Chennai, India

⁴ Electric Vehicles – Incubation, Testing and Research Centre, Vellore Institute of Technology, Chennai, India

Received: 11 January 2021 / Accepted: 10 September 2022

Abstract. The present work deals with steady state air flow analysis of electric motor having 20 hp rating running at 1450 rpm. The motor is being used to run the belt pull system to drive the exhaust fan in the industry. Air flow analysis of electric motor is carried out to predict temperature distribution over the motor. The modeling of the complete motor is done in CATIA. Meshing of whole geometry is done in ICEM CFD14.5. Results are obtained using FLUENT. In this research only copper losses and iron losses are taken into consideration based on the output obtained from electrical simulation software. The copper and iron losses are found out from electromagnetic analysis using Motorsolve software. Losses are treated as heat source or input to find out temperature distribution. To improve the accuracy, the computational fluid dynamics (CFD) analysis is performed by considering the air flow around casing and fins and thermal generation due to the losses. It is observed that there is a significant rise in temperature on casing and on fins for 30 °C ambient temperature.

Keywords: Steady state / CFD / electromagnetic analysis / temperature distribution

1 Introduction

Induction motor (InM) is used for more than 80% of the applications worldwide. These machines are affected by various electrical and mechanical unbalances which reflect in the losses and subsequent increase in temperature affects the life expectancy of the machine [1]. Due to this, the possibility of failure must be considered in the mechanical investigation to confirm the good working of the system [2]. Thermal modelling is a complex procedure [3,4]. The assessment of losses in InM is essential, as it directly impacts the temperature distribution and also the efficiency [5]. In InM, the electromagnetic losses such as ohmic losses and core losses act as the source of thermal generations. For an efficient and safe functioning of the motor, significant concern has to be taken to study these generations.

Ingersoll Rand et al. [6] studied how performance of screw compressor is influenced with change in temperature distribution of electric motor which is used to run screw compressor. Temperature distribution is carried out with the help of thermocouples and computational fluid dynamics (CFD) analysis. But according to this study, the thermal profile can be evaluated better using CFD

analysis than experimental studies using thermocouples because CFD analysis helps easily to discover hot spots in motor. Jerzy et al. [7] carried out air flow analysis of motor. They analysed two types of fans as well as two types of fan covers to improve its cooling efficiency. An analysis of the construction was carried out by CFD method using Autodesk Simulation CFD 2013. He concluded that the better solution for machines with fixed direction of rotation is to be used instead of the axial fan. For axial fan the motor temperature in the same condition was lower by about 5 °C.

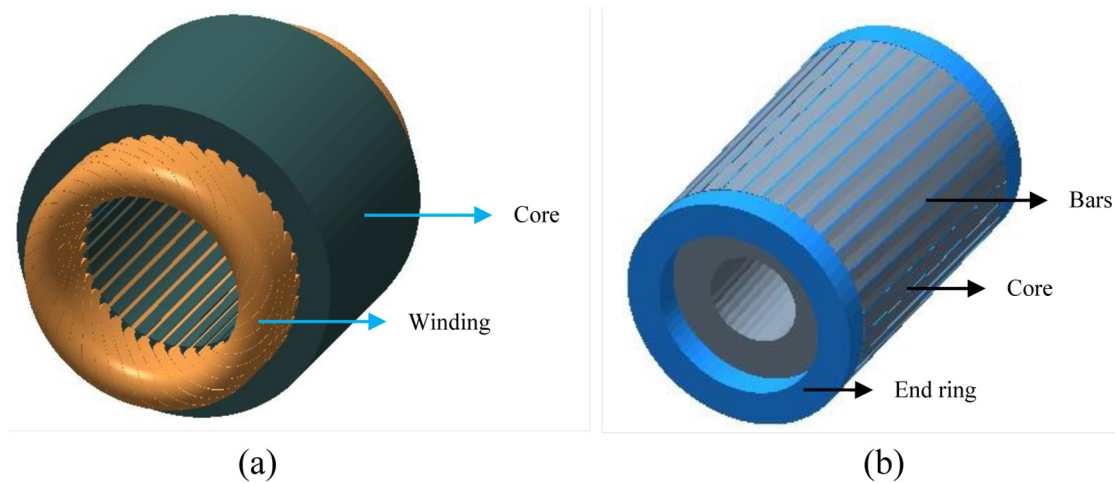
Numerous fluid analyses of the motor are centered on local fluid field, while research towards whole fluid space, particularly for small and medium size induction motors are less especially with centrifugal impeller [8–10]. The threshold of the sizing and motor operation is mainly decided by the temperature developed. When the temperature is high, necessary cooling methods are required to be implemented. Designing the motor with proper sizing and provide necessary cooling method is made possible with accurate thermal evaluation playing a major role.

In this thermal study, to improve the accuracy, the computational fluid dynamics (CFD) analysis is performed [11]. The electrical losses such as winding losses and core losses are only considered, as they constitute of 90–95% of the total losses. An InM with power rating of 20 hp/15 kW and line current rating of 29 A is considered for the case study.

* e-mail: lenin.nc@vit.ac.in

Table 1. Motor specifications and modeling.

Output power	15 kW
Line voltage	415 V
Rated speed	1450 RPM
Poles	4
Stator slots	36
Rotor bars	33
Winding type	Distributed
Connection type	Delta

**Fig. 1.** Electromagnetic analysis model (a) stator (b) rotor.

The rectangular fins are used as heat sink and there are 41 such fins on the motor casing. The forced cooling of InM is done by using fan placed on the rotor shaft which forces the air to flow on casing and the fins of the motor. Due to thermal generations as a result of the losses, the effectiveness of the external fin on the casing, air flow over the casing and fins, and the temperature rise under this condition will be the interest of this study. The CFD analysis of the machine is carried out using Ansys FLUENT [12,13].

2 Methodology

2.1 Air flow analysis in CFD

The losses act as heat generating source inside the motor which results in temperature rise of motor. These generated temperatures are dissipated by natural or forced convection. A cooling fan plays an important role in keeping temperature of motor by providing forced convection to cool down the motor. In this case, air is working as forced cooling medium. It is not possible to keep all the parts in the motor within desired temperature. Hence thermal behavior of external fins is also part of interest of this study. An electromagnetic analysis is done to find out losses. A computational domain is created, necessary boundary conditions and materials properties are incorporated and the CFD analysis [14] is carried out in Ansys FLUENT.

2.2 Electromagnetic analysis

Electromagnetic analysis is carried out to find out the losses in the motor using Motorsolve software. In InM, losses are classified as Iron or core loss and copper or ohmic losses. Iron or core losses are further divided as eddy current losses and hysteresis losses. As mentioned earlier other losses such as frictional, windage and stray load losses are very less as compared to core or Iron losses hence they are neglected. Following data in Table 1 is used to design the InM.

The motor in Figure 1 is designed with 36 slots in the stator and 33 rotor bars. Transformer steel is used as the core material for both stator and rotor. The winding is done with copper coils (density 8954 kg/m^3 , thermal conductivity of 386 W/mK and specific heat of 383.1 J/kgK). The rotor cage (bars and end rings) is made up of aluminum (density 2719 kg/m^3 , thermal conductivity of 202.4 W/mK and specific heat of 871 J/kgK).

Figure 2 shows CAD model of electric motor modeled using CATIA. Motor used for the study is 15 kW/ 20 hp at 1450 rpm. The motor is used to drive the belt pull system to drive the exhaust fan in the industry. A standard IEC Frame size 160 L is considered and the total number of poles is 4. Extension of shaft is 110 mm and diameter of shaft is 42 mm. Motor runs at 1450 rpm and rated torque is 98 Nm. The total number of fins taken for this study is 41.

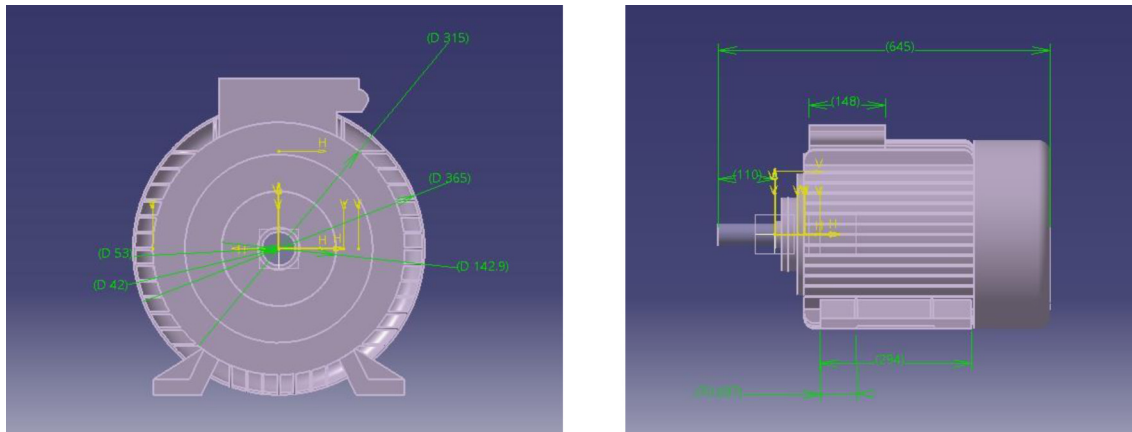


Fig. 2. CAD model of electric motor.

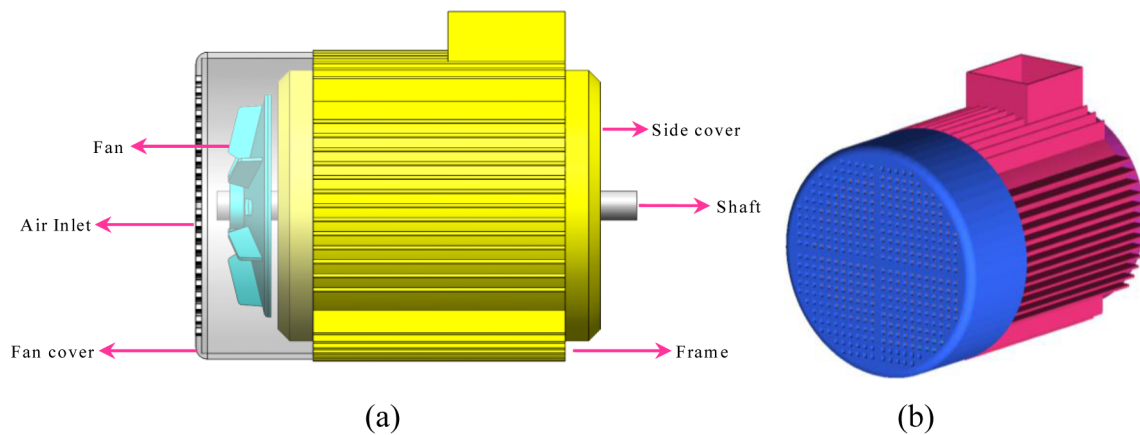


Fig. 3. Computational model; (a) side view, (b) ICEM CFD model.

2.3 Computational details

The computational domain in [Figure 3](#) is created in ICEM CFD [15]. Sufficient care is taken in creating the computational domain since the flow is external.

Meshing is the discretization of geometry where partial differential equation is applied to each element or cell. Equations are approximated over the elements (cells or zones) which are space partitions. Zone boundaries can be free to create computationally best shaped zones, or they can be fixed to represent internal or external boundaries within a model.

[Figures 4](#) and [5](#) show meshing of geometry without outer domain and with outer domain. Meshing is done using ICEMCFD software. Tetrahedral volume mesh is used for meshing. Mesh quality is dictated by the required accuracy. The quality achieved is between 0.1 and 0.2. After some trial and errors, fine mesh is obtained. The total number of elements is 1.6M.

There is no one turbulence model which is universally accepted as superior for all classes of problems. The choice of turbulence model will depend on considerations such as

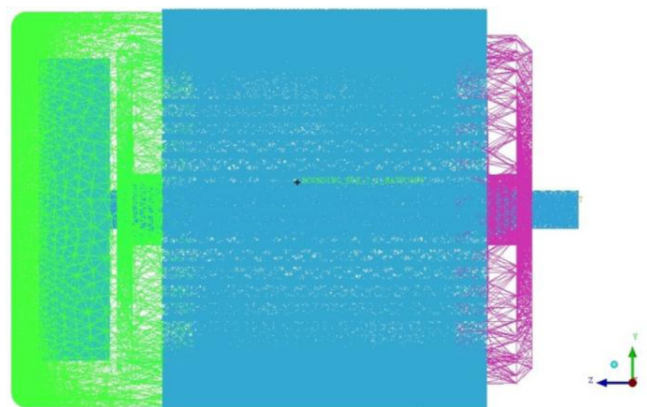


Fig. 4. Meshing of geometry without outer domain.

the level of accuracy required, physics encompassed in the flow, the available computational resources, the established practice for a specific class of problem and the amount of time available for the simulation. In the present work, *Shear stress transportation (SST) $k-\epsilon$* model has been

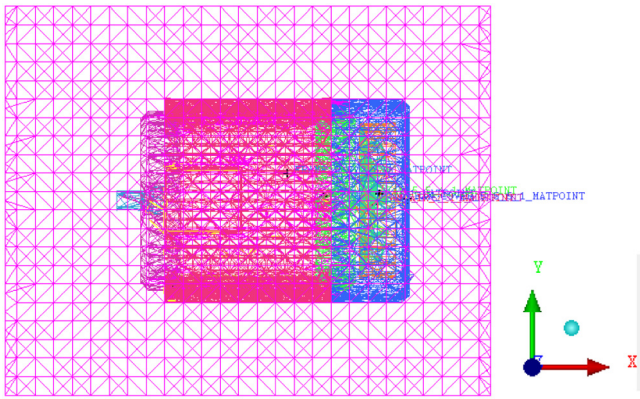


Fig. 5. Meshing of geometry with outer domain.

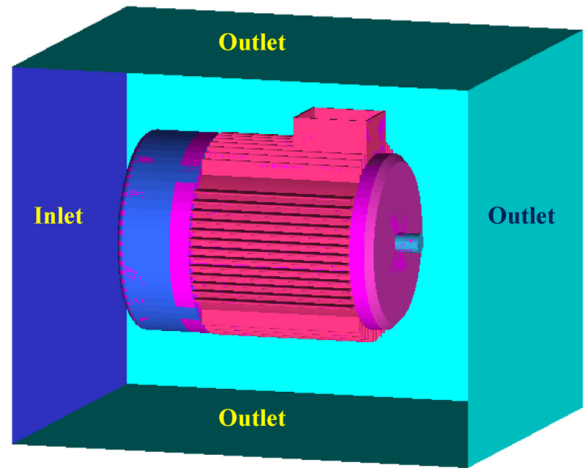


Fig. 6. Boundary conditions.

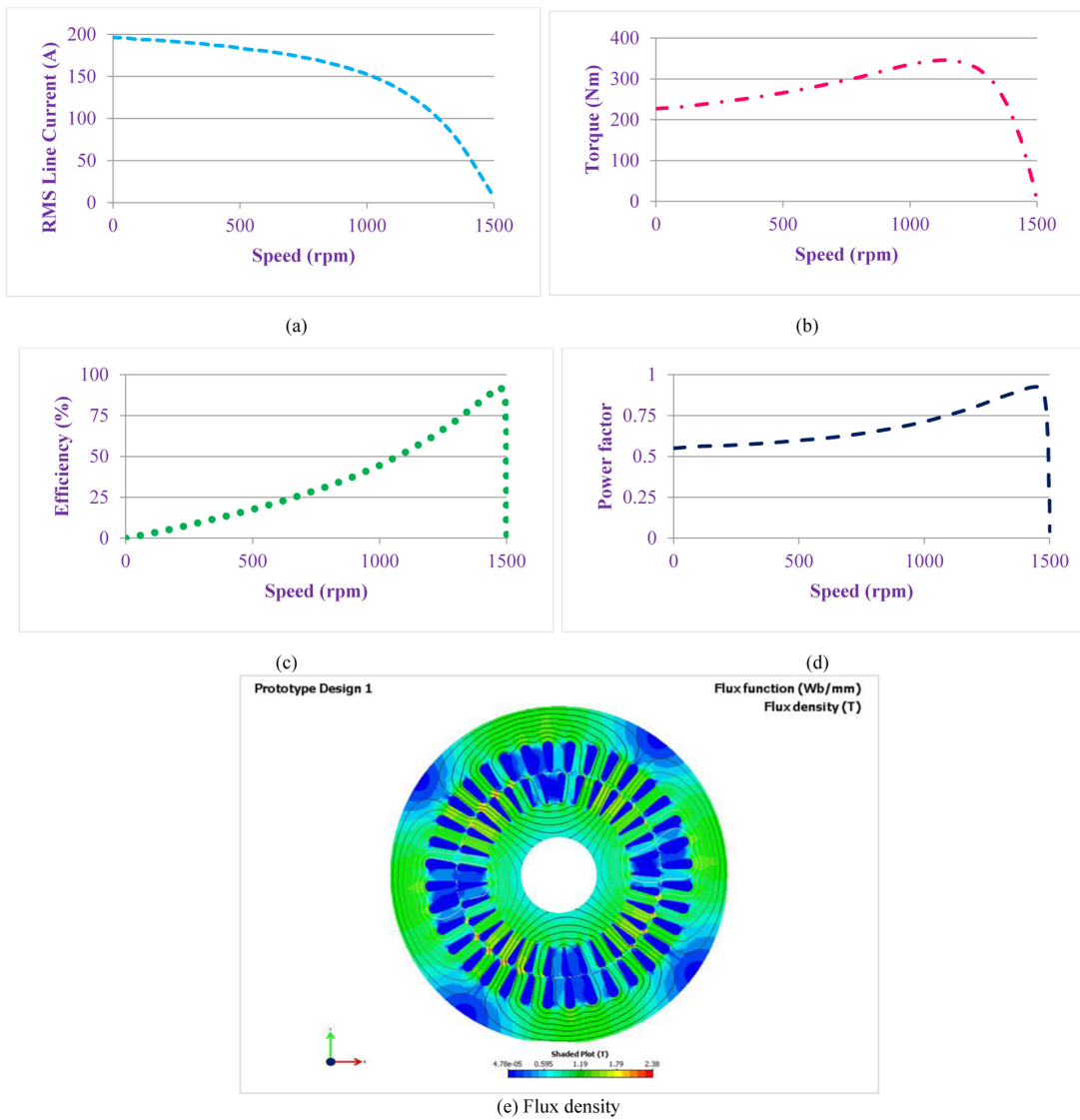


Fig. 7. Steady state results of 15 kW InM, (a) RMS line current vs speed, (b) torque vs speed, (c) efficiency vs speed, (d) power factor vs speed, (e) flux density plot at rated load.

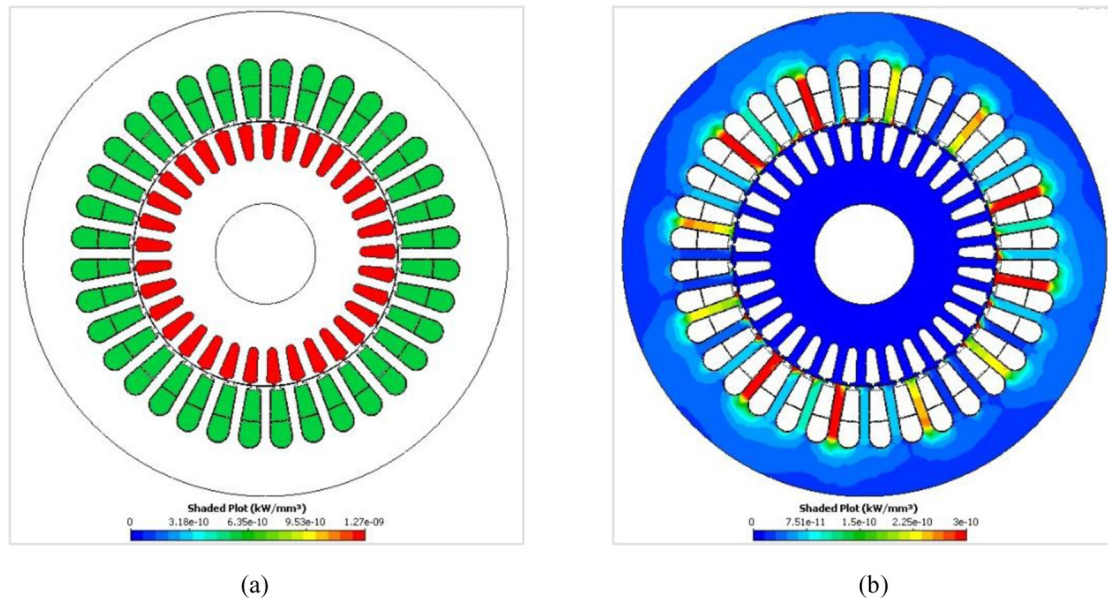


Fig. 8. Loss plots: (a) ohmic loss, (b) core loss.

used for the 3D calculations. This model accounts for principal turbulent shear stress considering free-stream independence in the far field providing the accuracy in computational region. Pressure outlet boundary condition is applied to all the sides of the outer domain except the bottom. The bottom side of the outer domain is given with wall boundary condition. Figure 6 shows the details of boundary conditions imposed on the model [16].

Air is the working fluid which is present in the space between stator and casing, hence convection heat transfer occurs. Copper and iron losses are applied on stator will create increase in temperature of stator and due to convection heat will get transferred to motor casing and fins of the motor. But due to cooling, fan temperature of casing and fin will decrease. Hence if we use more number of fins greater will be the temperature reduction of motor casing. In this analysis air flow over the motor is observed and also the temperatures on casing and fins.

3 Results and discussion

The resulting parameters in the analysis are plotted in Figure 7 with respect to speed of the motor. The steady state results provide the characteristics of the InM. From the results it is observed that at 1450 rpm, the InM has produces 98.4 Nm torque with RMS line current of 29.2 A, having a power factor of 0.93. The flux density plot at rated load (Fig. 7e) depicts the distribution of the flux lines and flux density in the motor core.

The copper loss of 5.7 kW and the iron loss of 0.9 kW obtained from Figure 8 will be input for the CFD analysis. The respective copper and iron losses are applied on conductor and core of motor respectively as loss density to respective conductor (Stator winding and rotor cage) and core bodies (stator and rotor core). Material used for motor casing is cast iron.

The CFD results are taken from FLUENT after the convergence with residuals of thermal, and air velocity with a precision of 10^{-6} is achieved [17]. Figure 9 shows the velocity and air flow pattern over the motor. Flow starts at the inlet of the motor continue over the motor. No air is allowed to flow through the motor.

Figures 10 and 11 show the temperature distribution along the casing of motor and the fins. If we consider fins, bottom portion of all fins are having more temperature than upper edge of fins as the bottom of fins is directly connected to casing which is the heat generating source. The fin temperature observed is around 315 K. If we consider motor casing, temperature observed is around 342 K i.e. around 69 °C.

From this analysis one can know where the temperature is high as it can harm for stator windings which leads to motor failure because working temperature of motor is directly related to life span of motor. Figure 12 shows temperature distribution for overall motor. It indicates the fan cover and the inlet there is very less temperature rise. The temperature observed on inlet is around 306 K and maximum temperature observed is 350 K. But portion beyond the fan cover there is considerable temperature rise. Near the fins and casing maximum temperature rise occurs due to heat losses. Again moving towards motor shaft, temperature rise is comparatively low.

The study could compute the various losses using electromagnetic analysis and the output could be used in a CFD study. The study showed the present design of the motor showed increase in temperature distribution on the casing and fins but less in the fan cover and inlet. The efficiency of the machine is determined by the thermal design of the motor. Further studies on various scenarios the motor may face higher temperature conditions is being studied, which could help in the prediction of the failure and can be used to activate a fail-safe condition for various applications.

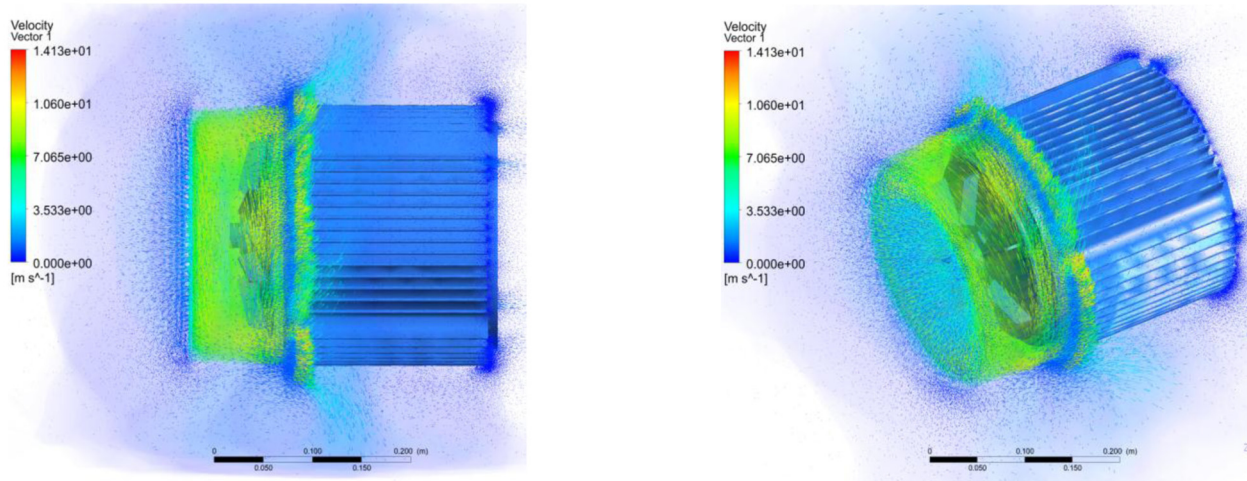


Fig. 9. Air flow over InM.

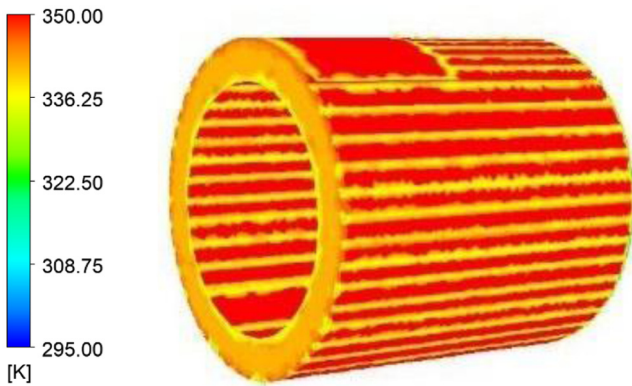


Fig. 10. Temperature distribution on casing.

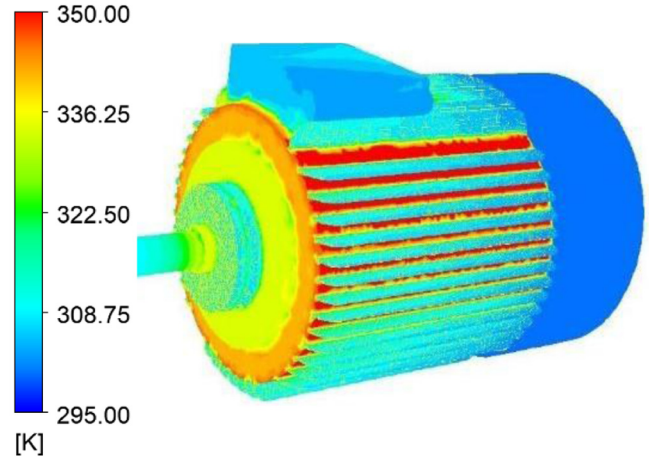


Fig. 12. Overall temperature distribution of motor.

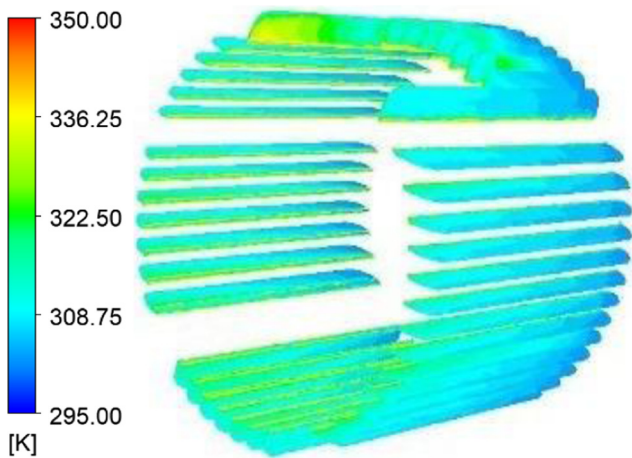


Fig. 11. Temperature distribution on fins.

4 Conclusion

In this paper, the InM is electromagnetically analysed and the losses are obtained. These losses are further applied in the CFD analysis to study the temperature rise on the casing and on the fins. Air flow over the motor is observed to evaluate the temperature variation more accurately. Also overall temperature distribution is observed. There is not much temperature rise on fan cover and inlet.

At the ambient temperature of 30 °C:

- The 15 kW InM is thermally studied at its rated condition of 415 V, 29 A with rated speed of 1450 rpm and rated torque of 98 Nm.
- The losses obtained from electromagnetic analysis are in the form of copper losses and iron losses which are 5.7 kW and 0.9 kW respectively.

- Percentage rise in temperature for casing is around 13%.
- Percentage temperature rise for fins is approximately 4%.
- The final temperature observed on the casing is 69 °C and on the fins it is 42 °C.
- On the casing there is 39 °C rise in temperature. Similarly for fins there is 12 °C rise.

From the above results, in steady state, it is clear that the temperature rise due to copper and core losses depends on the current through the conductors and the flux through core respectively.

References

1. A. Adouni, A.J.M. Cardoso, Thermal analysis of low-power three-phase induction motors operating under voltage unbalance and inter-turn short circuit faults, *Machines* **9**, 1–11 (2021)
2. B. Groschup, M. Nell, F. Pauli, K. Hameyer, Characteristic thermal parameters in electric motors: comparison between induction and permanent magnet excited machine, *IEEE Trans. Energy Convers.* **36**, 2239–2248 (2021)
3. B. Radi, A. Makhoulfi, A. El Hami, M. Sbaa, Optimization safety factors to study an ultrasonic motor, *Int. J. Simul. Multidiscip. Des. Optim.* **4**, 71–76 (2010)
4. D.G. Dorrell, D.A. Staton, J. Kahout, D. Hawkins, M.I. McGilp, Linked electromagnetic and thermal modelling of a permanent magnet motor, in *2006 3rd IET International Conference on Power Electronics, Machines and Drives – PEMD 2006* (2006), pp. 536–540
5. E. Gundabattini, R. Kuppan, D.G. Solomon, A. Kalam, D.P. Kothari, R. Abu Bakar, A review on methods of finding losses and cooling methods to increase efficiency of electric machines, *Ain Shams Eng. J.* **12**, 497–505 (2021)
6. S. Branch, A CFD study of screw compressor motor cooling analysis, *IOP Conf. Ser. Mater. Sci. Eng.* **232** (2017)
7. B. Będkowski, J. Madej, The potential of 3D FEM and CFD methods for cooling systems analysis of electrical machines – the premises, *Masz. Elektr. Zesz. Probl.* **1**, 139–143 (2012)
8. H. Li, Flow driven by a stamped metal cooling fan – numerical model and validation, *Exp. Therm. Fluid Sci.* **33**, 683–694 (2009)
9. H. Li, Cooling of a permanent magnet electric motor with a centrifugal impeller, *Int. J. Heat Mass Transf.* **53**, 797–810 (2010)
10. Y. Xie, J. Guo, P. Chen, Z. Li, Coupled fluid-thermal analysis for induction motors with broken bars operating under the rated load, *Energies* **11** (2018)
11. A. Boglietti, S. Nategh, E. Carpaneto, L. Boscaglia, C. Scema, An optimization method for cooling system design of traction motors, in *2019 IEEE Int. Electr. Mach. Drives Conf. IEMDC 2019* (2019), pp. 1210–1215
12. W. Kelly, B. Gigas, Using CFD to predict the behavior of power law fluids near axial-flow impellers operating in the transitional flow regime, *Chem. Eng. Sci.* **58**, 2141–2152 (2003)
13. C.-C. Chang, Y.-F. Kuo, J.-C. Wang, S.-L. Chen, Air cooling for a large-scale motor, *Appl. Therm. Eng.* **30**, 1360–1368 (2010)
14. B.N. Murthy, N.A. Deshmukh, A.W. Patwardhan, J.B. Joshi, Hollow self-inducing impellers: flow visualization and CFD simulation, *Chem. Eng. Sci.* **62**, 3839–3848 (2007)
15. ANSYS ICEM CFD 11.0 Tutorial Manual, Ansys, 2012. [Online]. Available: <https://engineering.purdue.edu/~scalomenu/teaching/me608/tutorial.pdf> [Accessed: 18 December 2021]
16. Standard and SST k- ω omega Models, Ansys Fluent, 2009. [Online]. Available: <https://www.afs.enea.it/project/neptunius/docs/fluent/html/th/node65.htm> [Accessed 18 December 2021]
17. ANSYS FLUENT 12.0 User's Guide – 26.18.1 Judging Convergence, Ansys (2009)

Cite this article as: Anuprita Bhosale, Sathyanarayanan Nandagopal, Davidson Jebaseelan, Siva Kumar Ramasami, Lenin Natesan Chokkalingam, Air flow analysis of 20 hp three phase induction motor, *Int. J. Simul. Multidisci. Des. Optim.* **13**, 25 (2022)